Supplementary Information

Auto-SELEX: A Fully Automated Microfluidic Platform for Rapid Discovery of High-Affinity Aptamers

Yang Bu [a], Yuze Liu [b], Anni Hu [b], Yung Ching Lee [a], and Levent Yobas [a,b,]*

[a]Department of Electronic and Computer Engineering,

[b]Department of Chemical and Biological Engineering,

The Hong Kong University of Science and Technology,

Clear Water Bay, Hong Kong SAR, China

** Corresponding author. Address: CYT-3012, Cheng Yu Tung Building, The Hong Kong University of Science and Technology, Hong Kong SAR.*

Email: eelyobas@ust.hk; Phone: +852-2358 7068. Fax: +852-2358 1485

Contents:

SUPPLEMENTARY MOVIES

Movie S1. Video microscopy illustrating the Auto-SELEX workflow using food dyes to visualize fluid transport, where blue represents the sample (target-library mixture), red represents the PCR mix containing forward primers and AuNRs, green represents magnetic beads, and brown represents the elution buffer containing AuNRs. The video is played at 2 × the recorded speed.

Movie S2. Video fluorescence microscopy demonstrating continuous-flow electrophoretic separation of aptamer-IgE complexes from unbound ssDNA sequences through the 2D CW sieve under increasing electric field strengths applied orthogonal to the focused sample stream. The video is played at 2 × the recorded speed and corresponds to Fig. 3C in the main text.

SUPPLEMENTARY FIGURES

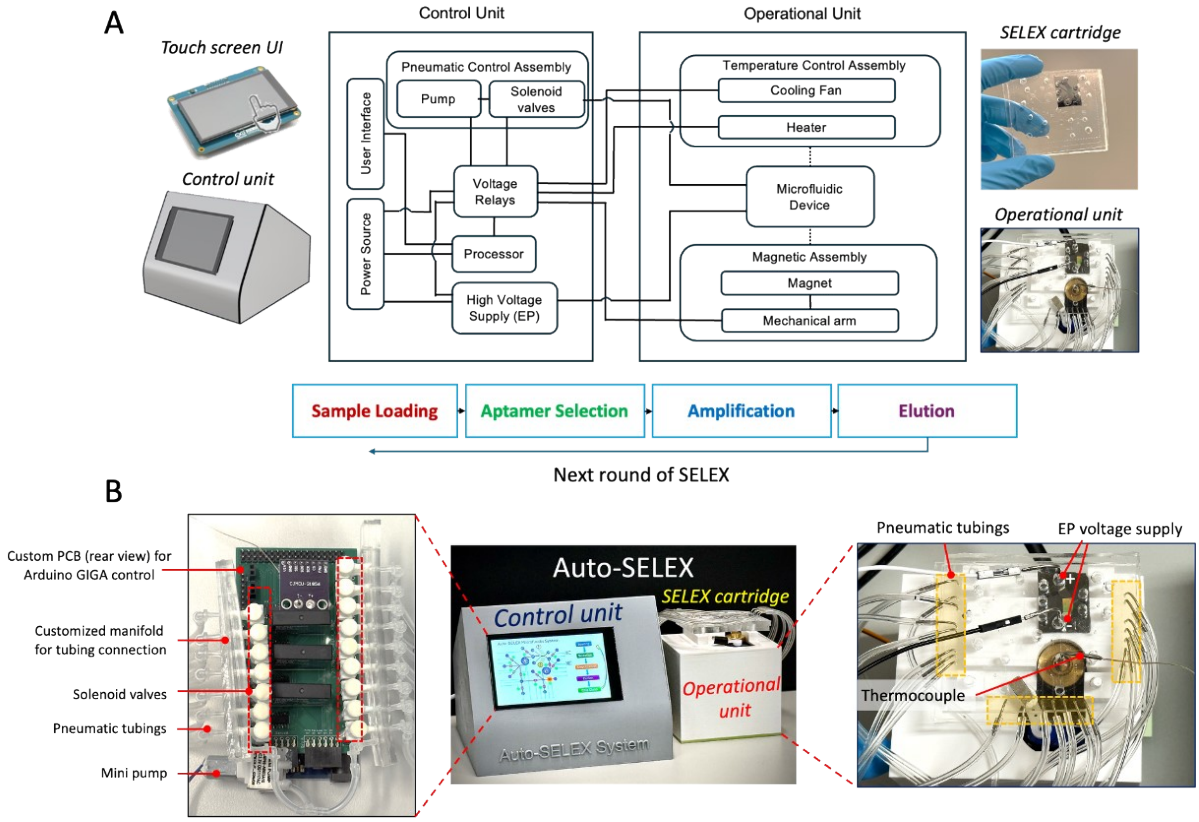

Fig. S1. Auto-SELEX system overview. (A) Block diagrams of the control and operational units highlighting the core components, key process steps, and photographs of the SELEX cartridge and operational unit. (B) Photographs of the Auto-SELEX system.

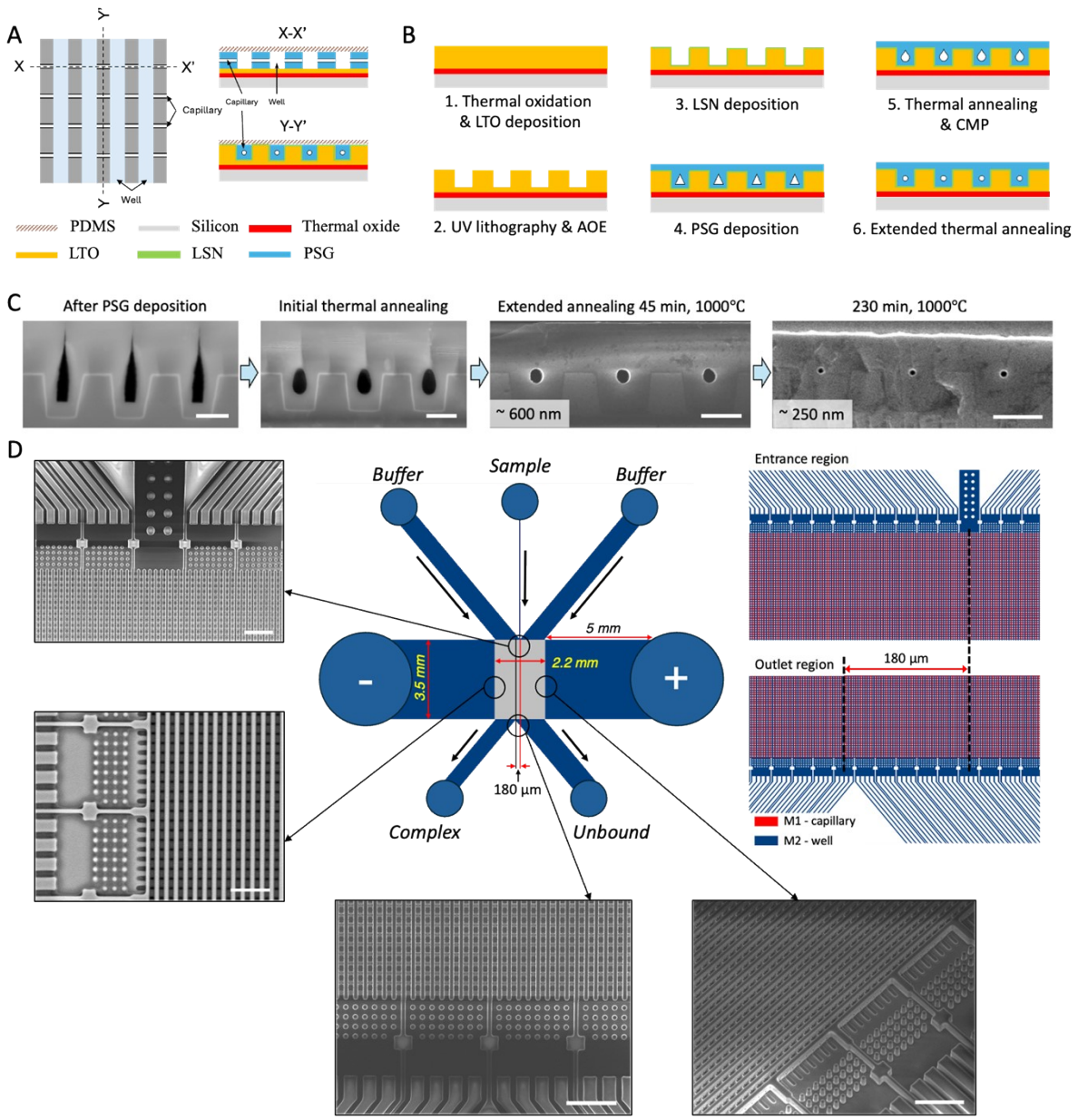

Fig. S2. Fabrication and design layout of the 2D CW sieve. (A) Schematic descriptions of the sieve array showing the top view and cross-sectional views of an array segment along the x- and y-axes. (B) Process flow diagrams in cross-sectional views illustrating the key fabrication steps. LTO: low-temperature oxide; LSN: low-stress nitride; CMP: chemical mechanical polishing; AOE: Advanced oxide etch; PSG: phosphosilicate glass. The second UV lithography step and subsequent AOE for forming the reservoirs and microchannels are not illustrated. (C) Scanning electron microscopy (SEM) images demonstrating tuning of the capillary diameter

through thermal annealing of PSG. Cross-sectional views of the sieve show three adjacent capillaries (self-enclosed channels) following PSG deposition, initial thermal annealing and then extended thermal annealing first for 45 min and subsequently for 230 min both at 1000 °C. Auto-SELEX system utilizes an optimized capillary diameter of ~700 nm. Scale bars: 2 μm. (D) Design layout with accompanying SEM images revealing microstructural details at various sieve sites. The inlet is aligned with the default outlet (Outlet II), while the alternative outlet (Outlet I) is laterally offset from the inlet by 180 μm. Scale bars: 20 μm.

1. Cap Layer

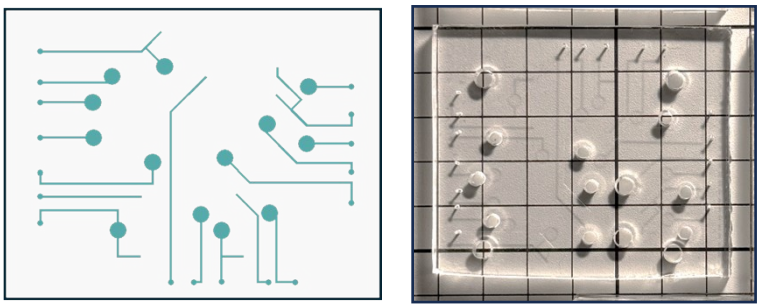

2. Pneumatic Layer

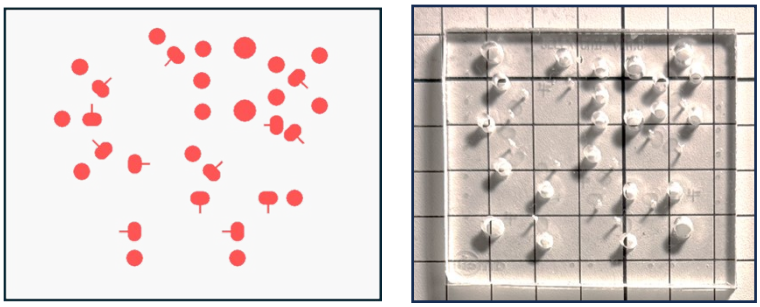

3. PDMS membrane

4. Fluidic Layer

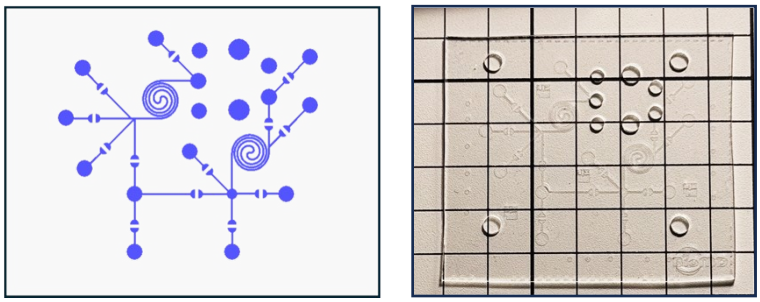

5. Capillary-well sieve

Assembled cartridge

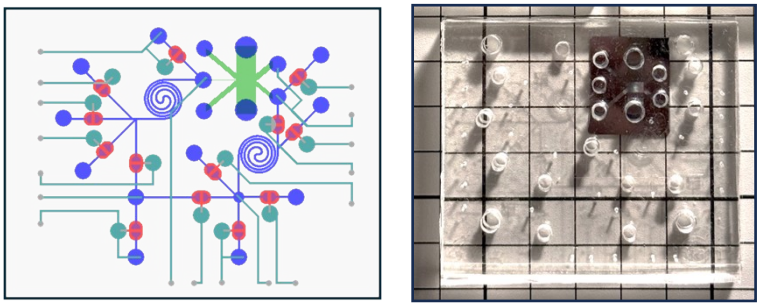

Fig. S3. Layouts of the cartridge layers (from top to bottom) and an assembled cartridge shown along with their pictures.

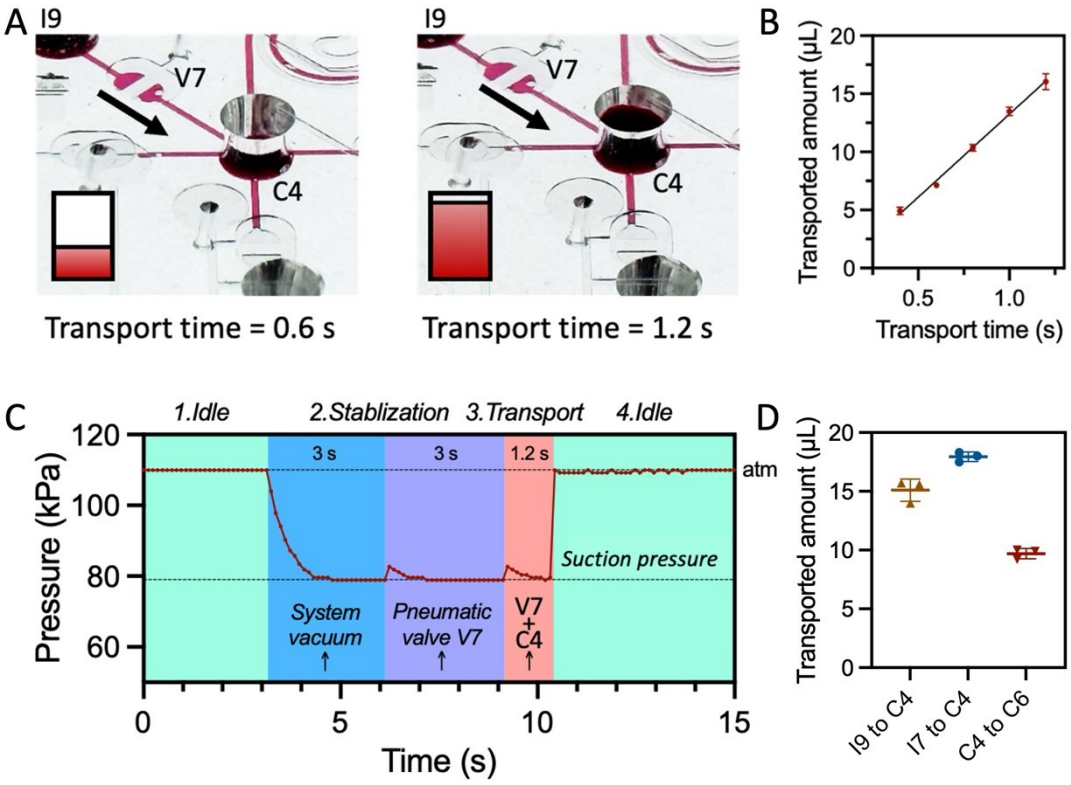

Fig. S4. Vacuum-driven liquid transfer within the cartridge. (A) Food dye (red) is transferred from reservoir I9 to the PCR chamber (C4) via valve V7. Sequential images show partial and near-complete filling of chamber C4 after transfer durations of 0.6 and 1.2 s, respectively. (B) The plot shows a linear relationship (R^2 = 0.99) between transferred volume and transfer duration (mean ± SD; n = 5). (C) The plot shows the vacuum profile applied during transfer. Liquid transfer is initiated by opening V7 followed by application of vacuum to chamber C4, and is metered by controlling the duration of concurrent vacuum application to V7 and C4, enabling programmable volumetric dosing. (D) The plot shows cartridge-to-cartridge reproducibility of transferred volume through three representative fluidic paths (I9 to C4 via V7, I7 to C4 via V4, and C4 to C6 via V8) under a fixed valve-opening duration of 1.2 s. Error bars represent standard deviations based on measurements from three independent cartridges.

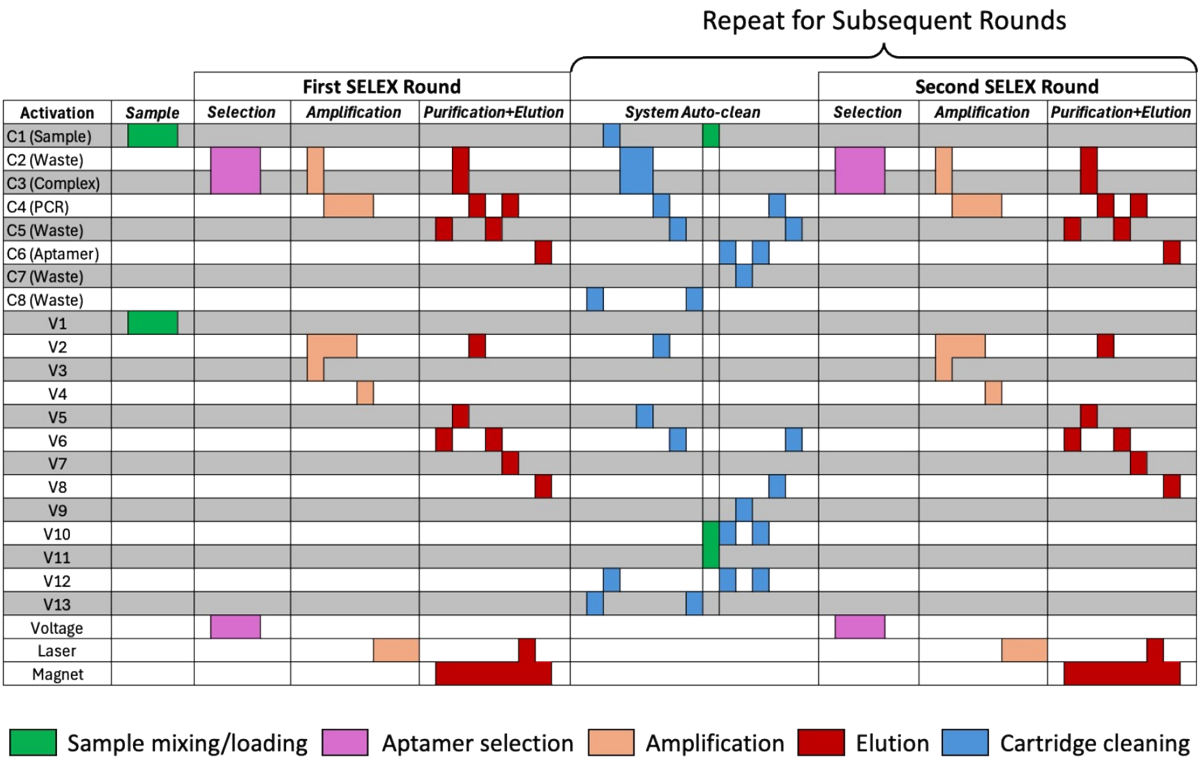

Fig. S5. Auto-SELEX workflow activation sequence.

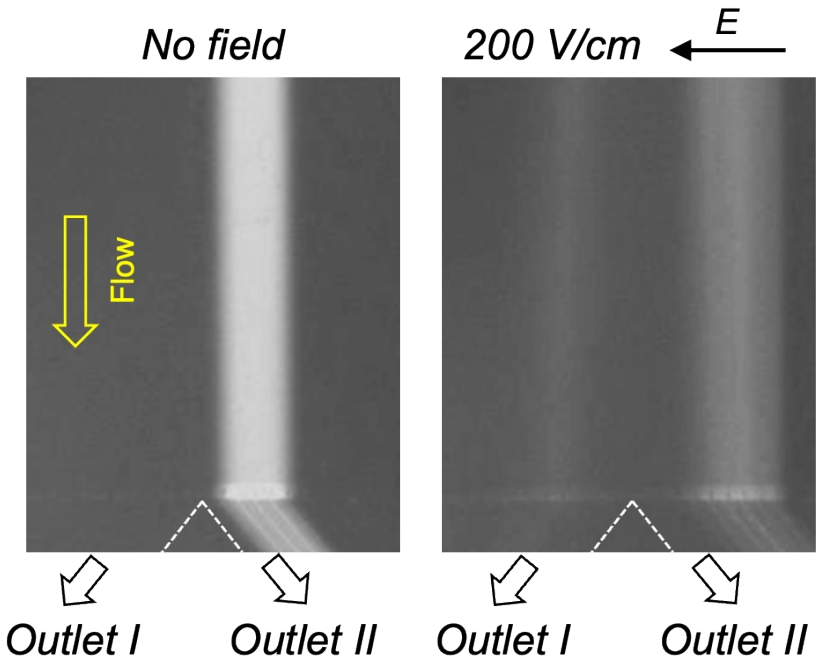

Fig. S6. Fluorescence images of a sample stream containing vitronectin (2 μM) and FAM-labelled randomized ssDNA library (2 μM) exiting the sieve in the absence and presence of an applied average electric field of 200 V/cm.

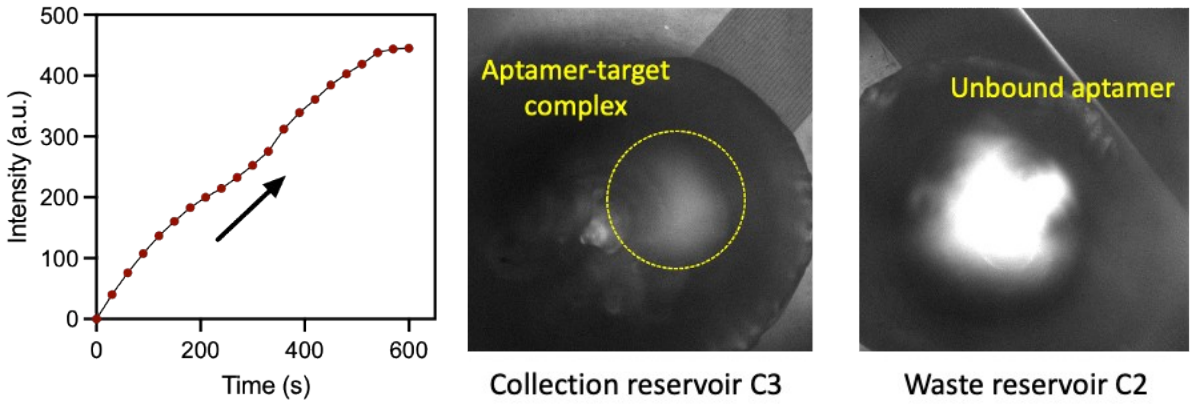

Fig. S7. Fluorescence images of chambers C2 and C3, respectively, accumulating unbound ssDNA strands and aptamer-IgE complex, acquired 5 min after the onset of continuous-flow separation through the sieve under an average electric field of 200 V/cm. The corresponding plot shows a monotonic increase in fluorescence intensity over time in chamber C3, indicating progressive accumulation of the aptamer-IgE complex over time.

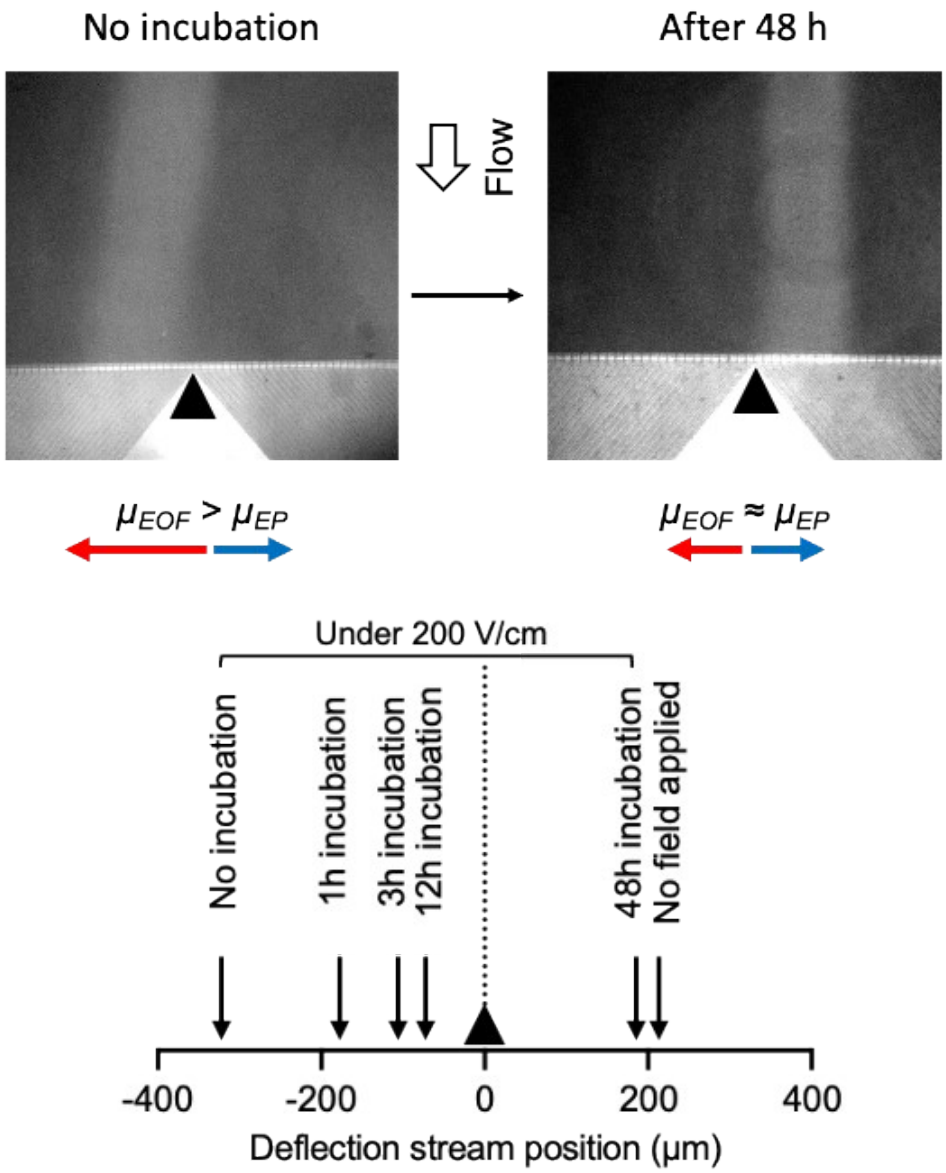

Fig. S8. Evolution of EOF with chip incubation duration in 1× TGK buffer under an applied average electric field of 200 V/cm. Representative fluorescence images show the stream exiting the sieve prior to chip incubation and after 48 h of incubation. The below diagram shows the deflection extent for the unbound ssDNA stream relative to the dashed line indicating the outlet bifurcation (arrowhead), as a function of chip incubation time.

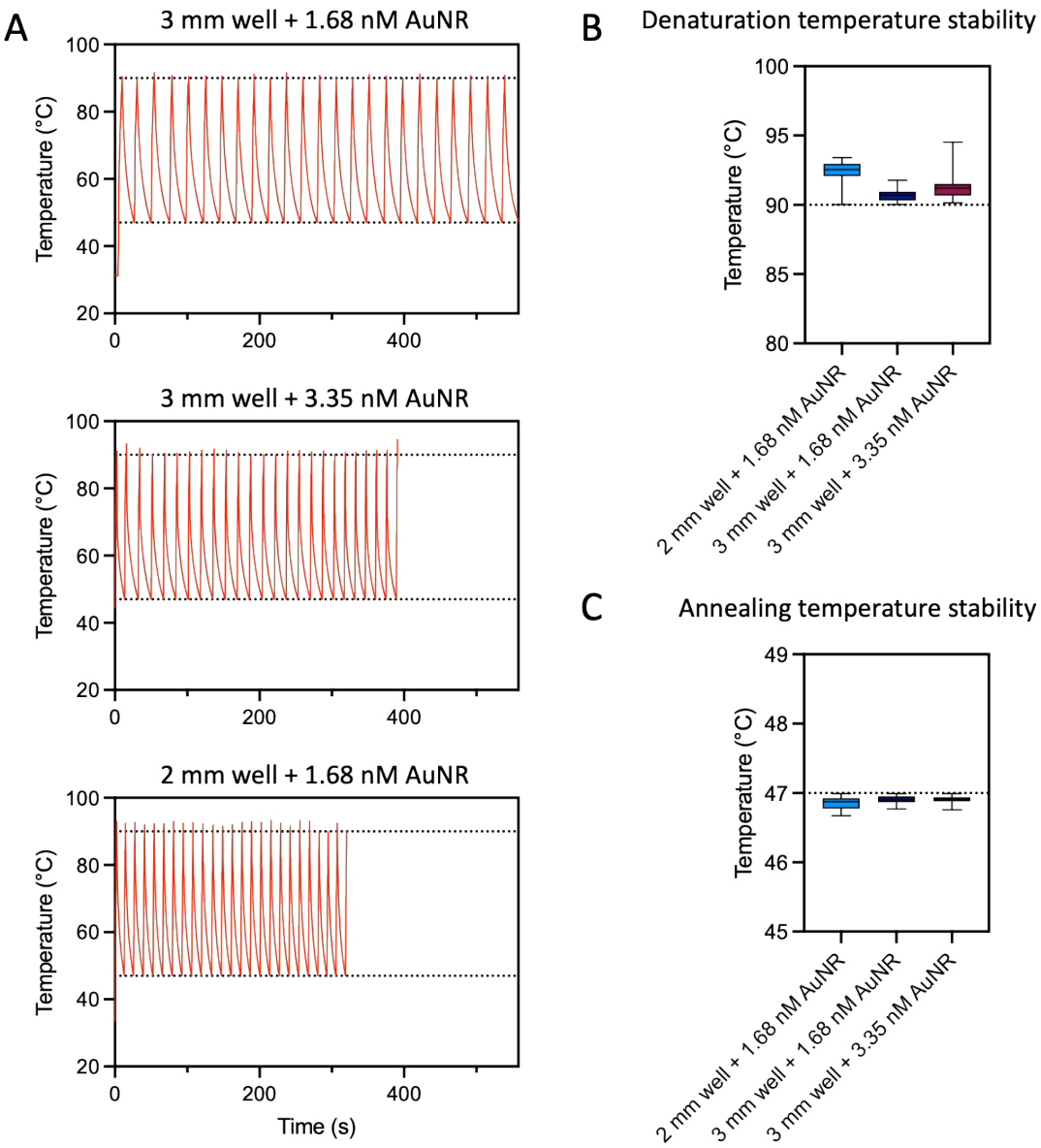

Fig. S9. Thermal cycling performance of bead-based plasmonic PCR within 2-mm- and 3-mm-diameter vacuum-driven chambers using 1.68 nM and 3.35 nM AuNRs. (A) Temperature profiles over 25 cycles. Cycle-to-cycle temperature stability during (B) denaturation (target: 92 °C) and (C) annealing/extension (target: 47 °C). The PCR chamber contains a 16 µL reaction mixture consisting of 1× KOD One™ PCR Master Mix supplemented with 1 µM FAM-labeled forward primer, 1.68 nM or 3.35 nM AuNRs, 5 nM ssDNA library template, and 60 µg reverse primer-functionalized magnetic beads.

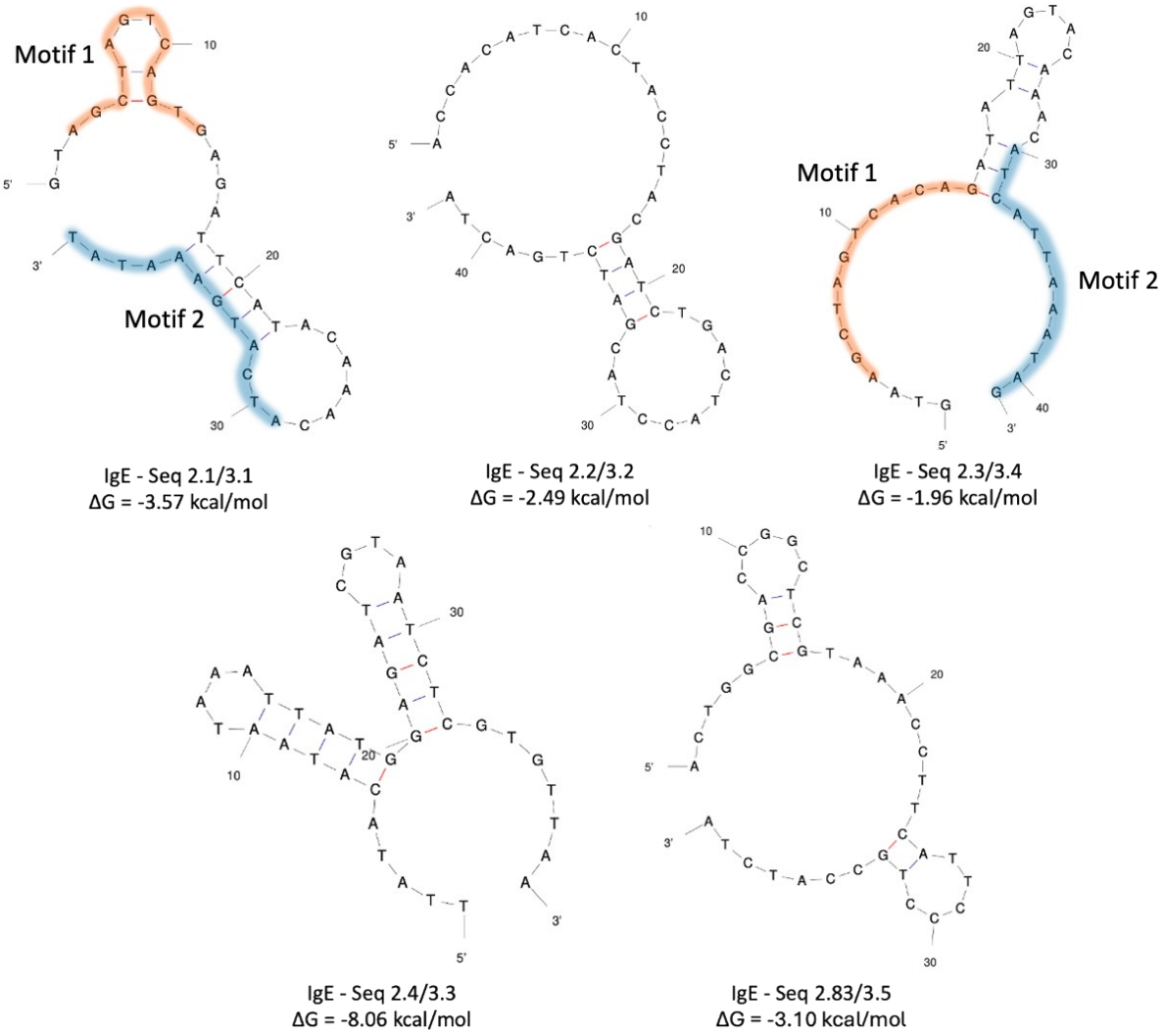

Fig. S10. Predicted secondary structures of selected aptamers against human IgE.

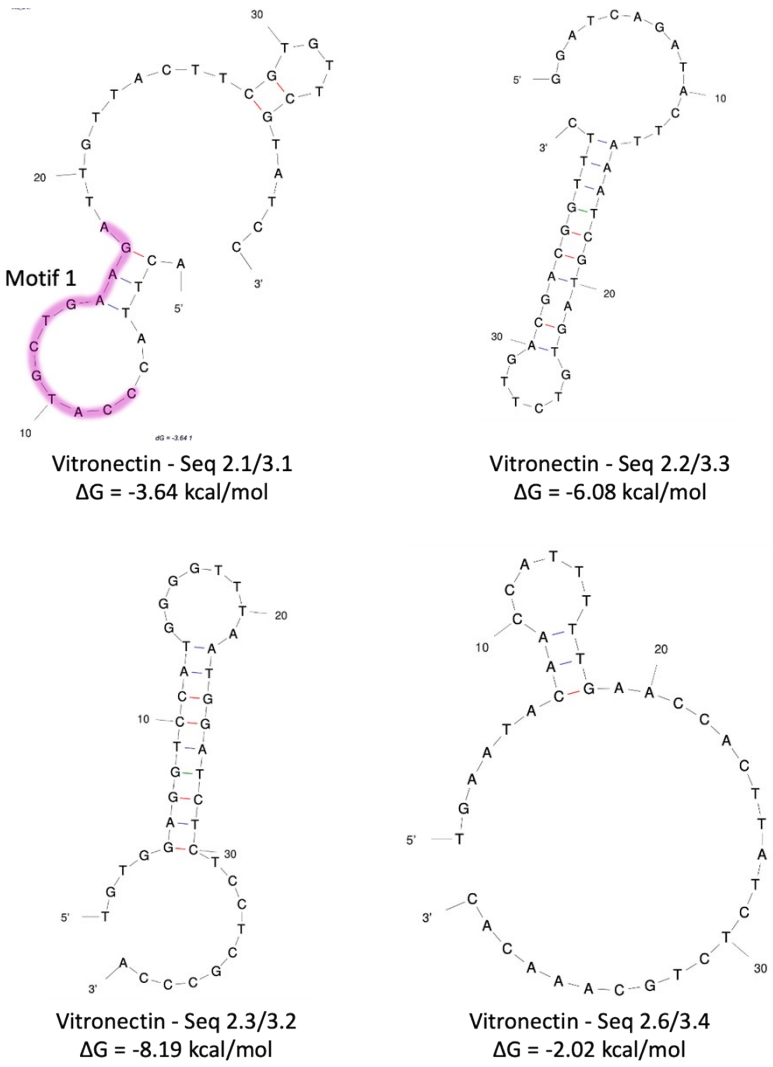

Fig. S11. Predicted secondary structures of selected aptamers against human vitronectin.

	Two-round selection	E-value	Three-round selection	E-value
IgE-motif 1		9.8e-185	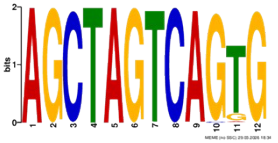	3.2e-708
IgE-motif 2	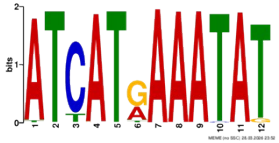	3.0e-009		1.7e-509
IgE-motif 3	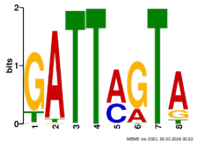	4.3e-212	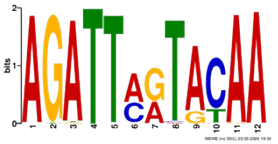	9.3e-445
Vitronectin-motif 1		2.8e-002		1.6e-017
Vitronectin-motif 2	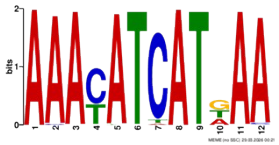	1.5e-019	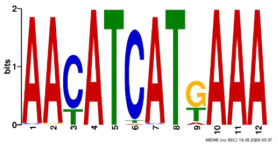	3.9e-128

Fig. S12. Sequence logos of motifs identified by MEME Suite from independent two-round and three-round selections. Motifs with E-values ≤ 0.05 are considered statistically significant (non-random); those with E-values $\leq 10^{-5}$ represent highly significant motifs indicating strong sequence conservation.

SUPPLEMENTARY TABLES

Table S1. Auto-SELEX cartridge reservoir loading before initiating the workflow.

Reservoir	Content	Composition & Concentration	Volume* (µL)
I1	Mixture of target protein & ssDNA library preincubated for 30 min (used in round 1)	IgE (50 nM) + Random ssDNA Pool (10 µM)	15
I2	Aptamer selection buffer	1× TGK	20
I3			
I4			40
I5			
I6	PCR reagents & AuNRs	2 × KOD Master Mix + Forward Primer (2 µM) + AuNR (3.35 nM)	20
I7	Reverse primer-modified magnetic beads (2.8 µm)	8.57 µg/µL in PCR water	20
I8	Wash buffer	1× TGK	80
I9	AuNRs (10 nm × 41 nm)	AuNR, 1.68 nM in 1× TGK	20
I10	Wash buffer	1× TGK	80
I11	Target protein (used in subsequent rounds)	IgE, 50 nM	30

*The listed volumes support the selection for two rounds and they scale proportionally for additional rounds.

Table S2. Sequencing read statistics for selected pools (length analysis is based on the random region with the expected length of 40 nt).

	Selection depth	Total reads	Reads 38–42 nt	% within 38–42 nt	Unique sequences	% Duplicate
Random Library	-	109,893	109,585	99.72%	100,205	8.56
IgE Pool	two-round	64,253	63,056	98.10%	51,968	17.58
	three-round	79,756	79,297	99.40%	53,447	32.60
Vitronectin Pool	two-round	150,581	149,571	99.30%	135,411	9.47
	three-round	122,512	121,288	99.00%	103,814	14.41

Table S3. Sequences of selected aptamers, without primer regions, against human IgE and vitronectin ranked according to their abundance expressed as reads per million (RPM). Aptamer binding affinity measurements exclude primer regions.

Target	No.	Sequence (5' – 3')	Two rounds (RPM)	Three rounds (RPM)	Binding affinity (nM)
IgE	2.1/3.1	GT**AGCTAGTCAGTG**AGATTCAT<u>ACAAAC</u>**<u>ATCAT</u>GAAATAT**	222	277	19.0 ± 1.95
	2.2/3.2	ACCACATCACTACCTACGATCTGACTACCTACGATCTGACTA	174	227	25.3 ± 0.7
	2.3/3.4	GTA**AGCTAGTCACAG**ATATTAG<u>TACAAAC</u>**<u>ATCATT</u>AAATAG**	127	151	25.3 ± 2.5
	2.4/3.3	TTATACATAATAAATTATGGAGATCGTAATCTCGTGTTAA	111	177	28.2 ± 0.8
	2.83/3.5	ACTGGCGACCGGCTCGTAAACCTTCATTCCCTGCCATCTA	16	100	19.9 ± 1.8
Vitronectin	2.1/3.1	ACTTAC**CCATGCTGAAGA**TTGTTACTTCGTGTTCGTATCC	134	330	98.5 ± 5.5
	2.2/3.3	GGATCAGATACTTAAATCGTAGTGTCTTGACGACGGTTTC	94	124	108 ± 2.6
	2.3/3.2	TGTGGAGGTCCATGGGGTTTAATGGATCTCTCCTCGCCCA	87	165	118 ± 9.5
	2.6/3.4	TGAATACAACCATTTTTGAACCACTTATCTCTGCAAACAC	67	115	157 ± 13

Table S4. Enriched sequence motifs identified in IgE and vitronectin pools after three-round selection and their expressed abundance as reads per million (RPM).

Target	Motif	Consensus sequence	Two-round		Three-round		Relative Abundance (three-round over two-round)
			Unique seq	Reads (RPM)	Unique seq	Reads (RPM)	
IgE	Motif 1	AGCTAGTCAGTG	121	2395	128	13509	5.64×
	Motif 2	ATCATGAAATAT	139	2783	89	11723	4.21×
	Motif 3	AGATTMRTACAA*	104	2165	93	11961	5.53×
Vitronectin	Motif 1	CCATSCTGWRGR#	28	2427	34	3215	1.32×
	Motif 2	AACATCATKAAA#	31	2513	32	3463	1.38×

*M = A/C, R = A/G
#S = G/C, W = A/T, R = A/G, K = G/T

Table S5. Performance benchmarking of fully and semi-automated microfluidic SELEX platforms

Ref.	Partitioning	Partitioning time per round (min)	PCR	PCR time per round (min)	Total time per round (min)	Rounds	Protein target: Aptamer Affinity (Kd)	Automation level
Auto-SELEX (this work)	Electrokinetic free-solution partitioning across artificial sieve	~17 (2 min separation + 15 min incubation)	Plasmonic bead-based PCR	~10 (25 cycles)	~30	3	IgE: 19.0 nM; Vitronectin: 98.5 nM	Fully automated
Hybarger et al., 2006	Solid-phase capture (target immobilized in microline)	~15 (10 min binding + 3 min elution + washing)	Heating block	~60 (40 cycles)	~200	1 (for validation)	Not reported	Fully automated
Huang et al., 2010	Magnetic beads (target immobilized)	10 (5 min incubation + 5 min washing)	On-chip microheaters	~45 (20 cycles)	60	5	CRP: 3.51 nM	Fully automated
Huang et al., 2012		~10 (incubation + washing)	Array-type microheaters	~42 (20 cycles)	60	6	AFP: 2.37 nM	Fully automated
Hilton et al., 2015		~90 (18 min incubation + 60 min washing + thermal elution)	Bead-based PCR by microheater	~30 (25 cycles)	~120	2	IgE: 83.9 nM (pool affinity)	Semi-automated
Kim et al., 2016		~55 (10 min incubation + 5 min elution + 15 min washing + 25 min transfer)		~45 (25 cycles)	~200	3	IgE: 10-18 nM; Small molecule: 1-2 μM	Semi-automated
Olsen et al., 2017a		~110 (30 min incubation + 40 min washing + 40 min elution / transfer)		~15 (20 cycles)	~240	2	IgA: Not reported	Semi-automated
Olsen et al., 2017b		~40 (estimated)		~25 (20 cycles)	~150	4	IgE: 12 nM	Semi-automated
Sinha et al., 2018		Not specified	Thermoelectric heater/cooler	~38 (20 cycles)	~96	8	NT-proBNP: 2.89 nM; hcTnI: 19.8 nM; Fibrinogen: 4.4 nM	Fully automated
Olsen et al., 2023		~60 (10 min incubation + 35-45 min washing + transfer)	Bead-based PCR by microheater	~15 (12 cycles)	~120	6	Rituximab: 35.8 nM; Patient M-Ig: ~36 nM	Semi-automated

Table S6. Bill of materials for the Auto-SELEX system and disposable cartridge.

Module	Item	Part Number / Source	Cost (USD)
Control Unit	Enclosure	In-house 3D printing	$30
	Arduino GIGA R1 WiFi, display shield, and custom PCB	Arduino (Ivrea, Italy); custom PCB in-house	$134
	Miniature pump	CJWP08-AB03A10 (Conjoin, Xiamen, China)	$3
	Pressure sensor	MPX5700AP (NXP Semiconductors)	$26
	Solenoid valves (total 17 units)	LHDA0533115H (The LEE Company, Westbrook, CT)	$1,282
	Tubings, connectors, and wiring	Cole-Parmer	$13
		Subtotal	$1,488
Operational Unit	Enclosure	In-house 3D printing	$26
	808-nm laser	Arm Laser, Shenzhen, China	$77
	Cooling fan	AFB0512MA (Delta Electronics, Taipei)	$2
	K-type thermocouple	Omega Engineering (Norwalk, CT)	$1
	Motorized magnet arm (SG90 servo + permanent magnet)	SG90 (TowerPro, Taipei); HuiLunTe Magnets, Jiangsu, China	$3
		Subtotal	$109
		Total (System)	$1,588
Disposable Cartridge	2D CW sieve (Per dozen chips on a 4-inch wafer)	In-house cleanroom	$16
	PDMS base and curing agent (~90 g)	Sylgard 184, Dow Corning (Midland, MI)	$11
	PDMS membrane (~300 μm thick)	Westru (Hangzhou, China)	$1
		Total	$28

REFERENCES

G. Hybarger, J. Bynum, R. F. Williams, J. J. Valdes and J. P. Chambers, *Anal. Bioanal. Chem.*, 2006, **384**, 191–198.

C. J. Huang, H. I. Lin, S. C. Shiesh and G. B. Lee, *Biosens. Bioelectron.*, 2010, **25**, 1761–1766.

C. J. Huang, H. I. Lin, S. C. Shiesh and G. B. Lee, *Biosens. Bioelectron.*, 2012, **35**, 50–55.

J. P. Hilton, T. Olsen, J. Kim, J. Zhu, T. Nguyen, M. Barbu, R. Pei, M. Stojanovic and Q. Lin, *Microfluid. Nanofluid.*, 2015, **19**, 795–804.

J. Kim, T. R. Olsen, J. Zhu, J. P. Hilton, K.-A. Yang, R. Pei, M. N. Stojanovic and Q. Lin, *Sci. Rep.*, 2016, **6**, 26139.

T. R. Olsen, C. Tapia-Alveal, K.-A. Yang, X. Zhang, L. J. Pereira, N. Farmakidis, R. Pei, M. N. Stojanovic and Q. Lin, *J. Electrochem. Soc.*, 2017, **164**, B3122–B3129.

T. Olsen, J. Zhu, J. Kim, R. Pei, M. N. Stojanovic and Q. Lin, *SLAS Technol.*, 2017, **22**, 63–72.

A. Sinha, P. Gopinathan, Y.-D. Chung, H.-Y. Lin, K.-H. Li, H.-P. Ma, P.-C. Huang, S.-C. Shiesh and G.-B. Lee, *Biosens. Bioelectron.*, 2018, **122**, 104–112.

T. R. Olsen, C. Tapia-Alveal, K. Wen, T. S. Worgall, M. N. Stojanovic and Q. Lin, *Biomed. Microdevices*, 2023, **25**, 3.